ATLAS NOTE

ATL-PHYS-PUB-2016-022

2nd October 2016

Prospects for a search for direct pair production of top squarks in scenarios with compressed mass spectra at the high luminosity LHC with the ATLAS Detector

The ATLAS Collaboration

Abstract

The current searches at the LHC have yielded a limited sensitivity to top squark pair production in scenarios with compressed mass spectra, where the top squark decays via $\tilde{t}_1 \rightarrow t\tilde{\chi}_1^0$. The reach at the high-luminosity phase of the LHC is expected to significantly extend beyond the current limits. This document presents benchmark studies targeting dileptonic final states with a parameterised simulation of the ATLAS detector, considering proton-proton collisions at a centre-of-mass energy of 14 TeV. Results are shown for an integrated luminosity of 3000 fb^{-1}.

1 Introduction

Supersymmetry (SUSY) [1–6] is one of the most studied extensions of the Standard Model (SM). It predicts new bosonic partners for the existing fermions and fermionic partners for the known bosons. If R-parity is conserved [7], SUSY particles are produced in pairs and the lightest supersymmetric particle (LSP) is stable, providing a possible dark matter candidate. To address the SM hierarchy problem [8–11], TeV-scale masses are required [12, 13] for the supersymmetric partners of the gluons (gluinos, $\tilde{g}$) and the top quarks (top squarks, $\tilde{t}$) [14, 15]. The SUSY partners of the charged (neutral) Higgs and electroweak gauge bosons mix to form the mass eigenstates known as charginos, $\tilde{\chi}^{\pm}_{l}$, $l = 1, 2$ (neutralinos, $\tilde{\chi}^{0}_{m}$, $m = 1, \ldots, 4$) where the increasing index denotes increasing mass. The scalar partners of right-handed and left-handed quarks, $\tilde{q}_{\mathrm{R}}$ and $\tilde{q}_{\mathrm{L}}$, mix to form two mass eigenstates, $\tilde{q}_1$ and $\tilde{q}_2$, with $\tilde{q}_1$ defined to be the lighter of the two.

Searches for direct pair production of the lightest top squark mass eigenstate ($\tilde{t}_1$) have been performed by the ATLAS [16–20] and CMS [21–26] collaborations. Searches for $\tilde{t}_1 \to t\tilde{\chi}^{0}_{1}$ have little sensitivity to scenarios where the lightest stop is only slightly heavier than the sum of the masses of the top quark and the $\tilde{\chi}^{0}_{1}$, due to the similarities in kinematics with SM top quark pair production ($t\bar{t}$). This family of models has been directly targeted with the analysis of spin correlations of $t\bar{t}$ events in dileptonic final states [17], or with ISR-based selections [20], excluding at 95% CL top squark masses between the top quark mass and 191 GeV and between 230 GeV and 380 GeV.

This note presents the expected discovery and exclusion reach for top squark pair production in R-parity conserving SUSY models analysing up to ~3000 fb^{-1} of proton–proton collision data at the High Luminosity LHC (HL–LHC) with $\sqrt{s}$=14 TeV. The top squark pairs are assumed to decay via $\tilde{t}_1 \to t\tilde{\chi}^{0}_{1}$, as shown in Figure 1, with both top quarks decaying leptonically. This choice is motivated by the interest in performing measurements of possible new phenomena exploiting this final state. Models with compressed mass spectra are targeted, complementing the prospects presented in [27].

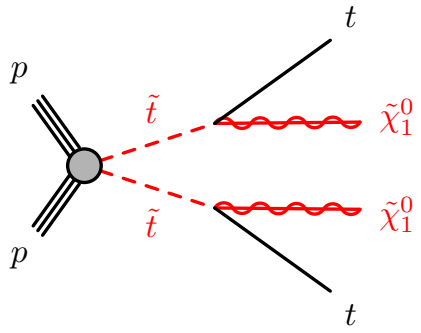

Figure 1: Diagram of the $\tilde{t}_1$ pair production process with $\tilde{t}_1 \to t\tilde{\chi}^{0}_{1}$ considered in this analysis prospect.

1.1 The LHC and HL–LHC

In the present data-taking period, the LHC will collect ~100 fb^{-1} of proton-proton collisions with an instantaneous luminosity of ~1×10^{34} cm^{-2}s^{-1} and an average number of collisions per bunch crossing of $\langle\mu\rangle \sim 25$. A second long shutdown (LS2) will follow, during which the injection chain is foreseen to be modified to allow for instantaneous luminosities up to ~2×10^{34} cm^{-2}s^{-1}. The average number of

proton-proton collisions per bunch crossing is expected to be $\langle\mu\rangle \sim 60$ and the data collected up to the next long shutdown (LS3) will amount to ~300 fb^{-1}. An increase of the centre-of-mass-energy to 14 TeV is possible and is assumed to happen for this study. During LS3, the accelerator is foreseen to be upgraded to the HL–LHC which will be able to achieve luminosities of ~7×10^{34} cm^{-2}s^{-1}. The HL–LHC is expected to deliver an average number of pile up interactions per bunch crossing of $\langle\mu\rangle \sim 200$ and the data collected will amount to ~3000 fb^{-1}.

2 ATLAS detector

The ATLAS experiment [28] is a multi-purpose particle detector with a forward-backward symmetric cylindrical geometry and nearly 4π coverage in solid angle[1]. The interaction point is surrounded by an inner detector (ID), a calorimeter system, and a muon spectrometer.

Upgrades to the detector and the triggering system are planned to adapt the experiment to the increasing instantaneous and integrated luminosities expected with the HL–LHC [29, 30].

In the reference upgrade scenario, the ID will provide precision tracking of charged particles for pseudorapidities $|\eta| < 4.0$ and will be surrounded by a superconducting solenoid providing a 2 T axial magnetic field. It will consist of pixel and silicon-microstrip detectors.

In the pseudorapidity region $|\eta| < 3.2$, the currently installed high-granularity lead/liquid-argon (LAr) electromagnetic (EM) sampling calorimeters will be used. The current steel/scintillator tile calorimeter will measure hadron energies for $|\eta| < 1.7$. The endcap and forward regions, spanning $1.5 < |\eta| < 4.9$, currently instrumented with LAr calorimeters for both the EM and hadronic energy measurements will be upgraded with a high granularity forward calorimeter in the $3.1 < |\eta| < 4.9$ range.

The muon spectrometer, consisting of three large superconducting toroids with eight coils each, a system of trigger and precision-tracking chambers, which provide triggering and tracking capabilities in the ranges $|\eta| < 2.4$ and $|\eta| < 2.7$, respectively, will be upgraded with the addition of a very forward muon tagger.

A two-level trigger system will be used to select events, reducing the event rate to about 10 kHz. In the reference scenario, the bandwidth allocated to single lepton (e or μ) triggers will be of ~ 2.2 kHz each, with the respective thresholds set at $p_{\mathrm{T}} > 22$ GeV and $p_{\mathrm{T}} > 20$ GeV.

3 Dataset and simulated event samples

Monte Carlo (MC) simulated event samples are used to predict the background from SM processes and to model the SUSY signal. The detector response is taken into account using a set of parameterised response functions based on studies performed with GEANT 4 simulations of the upgraded detector in high luminosity conditions. The most relevant MC samples have equivalent luminosities (at 14 TeV) of at least 3000 fb^{-1}.

[1] ATLAS uses a right-handed coordinate system with its origin at the nominal interaction point (IP) in the centre of the detector and the z-axis along the beam pipe. The x-axis points from the IP to the centre of the LHC ring, and the y-axis points upward. Cylindrical coordinates (r, ϕ) are used in the transverse plane, ϕ being the azimuthal angle around the beam pipe. The pseudorapidity is defined in terms of the polar angle θ as $\eta = -\ln\tan(\theta/2)$. Rapidity is defined as $y = 0.5\ln\left[(E + p_z)/(E - p_z)\right]$ where E denotes the energy and p_z is the component of the momentum along the beam direction.

For the production of $t\bar{t}$ and single top-quarks in the Wt channel [31], the Powheg-Box v2 generator [32–34] interfaced to the Pythia 8.186 [35] parton shower model is used. The A14 set of tuned parameters (tune) [36] is used together with the CT10 PDF set [37]. The top quark mass is assumed to be 172.5 GeV. The $t\bar{t}$ (single top) events are normalised to the NNLO + NNLL [38] (NLO) QCD cross-sections.

Samples of $t\bar{t}V$ (with $V = W$ and Z, including non-resonant Z/γ^* contributions) and $t\bar{t}WW$ production are generated at LO with MadGraph5_aMC@NLO [39] v2.2.2 interfaced to the Pythia 8.186 parton shower model, with up to two ($t\bar{t}W$), one ($t\bar{t}Z$) or no ($t\bar{t}WW$) extra partons included in the matrix element; they are described in detail in Ref. [40]. MadGraph5_aMC@NLO is also used to simulate the tZ, tWZ, $t\bar{t}t\bar{t}$ and $t\bar{t}t$ processes. The A14 tune is used together with the NNPDF23LO PDF set [41]. The $t\bar{t}W$, $t\bar{t}Z$, $t\bar{t}WW$ and $t\bar{t}t\bar{t}$ events are normalised to their NLO cross-sections [39] while the generator cross-section is used for tZ, tWZ and $t\bar{t}t$.

Events containing W and Z bosons with associated jets (W+jets and Z/γ^*+jets) are produced using the Sherpa v1.4.1 [42] generator with massive b/c-quarks to improve the treatment of the associated production of W and Z bosons with heavy flavour jets. The expected W+jets, Z+jets and diboson yields are normalised to the Sherpa predictions.

Diboson processes with four charged leptons (ℓ), three charged leptons and one neutrino, or two charged leptons and two neutrinos are simulated using the Sherpa v2.1.1 generator, and are described in detail in Ref. [43]. The matrix elements contain the WW, WZ and ZZ processes and all other diagrams with four or six electroweak vertices (such as same-electric-charge W boson production in association with two jets, $W^{\pm}W^{\pm}jj$). The CT10 parton distribution function (PDF) set is used for all Sherpa samples in conjunction with a dedicated tuning of the parton shower parameters developed by the Sherpa authors. The generator cross-sections (at NLO for most of the processes) are used when normalising these backgrounds.

Production of a Higgs boson in association with a $t\bar{t}$ pair is simulated using MadGraph5_aMC@NLO v2.2.2 interfaced to Herwig 2.7.1 [44]. The UEEE5 underlying-event tune is used together with the CTEQ6L1 [45] (matrix element) and CT10 (parton shower) PDF sets. Simulated samples of SM Higgs boson production in association with a W or Z boson are produced with Pythia 8.186, using the A14 tune and the NNPDF23LO PDF set. For normalisation purposes, cross-sections calculated at NLO [46] are used.

The SUSY signal samples are generated using LO matrix elements with up to two extra partons, with the MadGraph5_aMC@NLO v2.2.3 generator. The modelling of the SUSY decay chain, parton showering, hadronisation and the description of the underlying event are simulated with Pythia 8.186, using the A14 tune. Parton luminosities are provided by the NNPDF23LO PDF set. The jet-parton matching is realised following the CKKW-L prescription [47], with a matching scale set to one quarter of the pair-produced superpartner mass. Signal cross-sections are calculated to next-to-leading order in the strong coupling constant, adding the resummation of soft gluon emission at next-to-leading-logarithmic accuracy (NLO+NLL) [48–50]. The nominal cross-section and the uncertainty are taken from an envelope of cross-section predictions using different PDF sets and factorisation and renormalisation scales, as described in Ref. [51]. The production cross section of top squark pairs with a mass of 350 GeV and 700 GeV, which are used as benchmarks in this study, are respectively 4676 fb and 88 fb.

In all MC samples, except those produced by Sherpa, the EvtGen v1.2.0 program [52] is used to model the properties of the bottom and charm hadron decays.

4 Event selection

Candidate leptons are selected with p_{T} larger than 25 GeV to ensure that trigger efficiencies are constant in the relevant phase space, and $|\eta| < 2.47$ (2.4) for electrons (muons). They are also required to be isolated within the tracking volume: the scalar sum of the transverse momenta of charged tracks with $p_{\mathrm{T}} > 1$ GeV, not including the lepton track, within a cone of radius $\Delta R \equiv \sqrt{(\Delta\phi)^2 + (\Delta\eta)^2} = 0.2$ around the lepton candidate must be less than 15% of the lepton p_{T}, where $\Delta\eta$ and $\Delta\phi$ are the separations in η and ϕ.

Candidate jets are reconstructed with the anti-k_t algorithm with a radius parameter of 0.4. They are selected with $p_{\mathrm{T}} > 30$ GeV and $|\eta| < 2.5$ and requiring a tracking confirmation to reduce the contribution from pile-up. Signal events have been found to lie mostly in the central region of the detector, and the η requirements for leptons and jets, tighter than the detector acceptance, have been optimised accordingly.

Jets are required to be separated from candidate electrons by $\Delta R(e, \mathrm{jet}) > 0.2$. Leptons are removed if they are within $\Delta R = 0.4$ of a remaining jet. Jets are tagged as originating from b-decays (b-tagged) using a parameterisation (versus the jet p_{T} and η) modelling the performances of the MV1 b-tagging algorithm [53]. In simulated $t\bar{t}$ events, the chosen working point identifies b-jets with an average efficiency of 70%, for a c-jet misidentification probability of about 20% and a light-flavour jet misidentification probability of about 1%. The $E_{\mathrm{T}}^{\mathrm{miss}}$ at generator level is computed as the vectorial sum of the momenta of neutral weakly-interacting particles (neutrinos and neutralinos). It is then smeared to simulate the detector response, with a function parameterised in the average number of interactions per bunch crossing μ and the scalar sum of energy in the calorimeter $\sum E_{\mathrm{T}}$.

Events are accepted if they contain either exactly two electrons, two muons or one electron and one muon. Simulated events are reweighted by the expected efficiencies of the lepton trigger, reconstruction and identification. Furthermore, events are required to contain at least two b-jets from the $t\bar{t}$ decay.

The small mass splitting between the $\tilde{t}_1$ and $\tilde{\chi}_1^0$ implies that the top quark and the $\tilde{\chi}_1^0$ are generally produced with very small momentum, hence it is necessary to select events where the $\tilde{t}_1\,\tilde{t}_1$ system is boosted by the recoil of at least one energetic ISR jet. Since dileptonic final states are selected, the $\tilde{t}_1$ pair is identified by the two leptons and the two leading b-jets in the event. Each additional jet is assigned to the ISR system.

Different discriminators and kinematic variables are used in the analysis to separate the signal from the SM background.

- $\min\{\Delta\phi(\mathrm{jet}_{\mathrm{ISR}}, E_{\mathrm{T}}^{\mathrm{miss}})\}$: the minimum azimuthal angular distance between each jet assigned to the ISR system and the $E_{\mathrm{T}}^{\mathrm{miss}}$;
- $\Delta\phi(\mathrm{jet}_{\mathrm{ISR1}}, E_{\mathrm{T}}^{\mathrm{miss}})$: the azimuthal angular distance between the leading jet assigned to the ISR system and the $E_{\mathrm{T}}^{\mathrm{miss}}$;
- $R_{\ell\ell}$: the ratio of $E_{\mathrm{T}}^{\mathrm{miss}}$ and the scalar sum of the lepton transverse momenta;
- m_{T2}: lepton-based stransverse mass. The stransverse mass [54, 55] is a kinematic variable used to bound the masses of a pair of intermediate particles which are presumed to each have decayed semi-invisibly into one visible and one invisible particle. The stransverse mass is defined as

$$m_{\mathrm{T2}}(\mathbf{p}_{\mathrm{T},1}, \mathbf{p}_{\mathrm{T},2}, \mathbf{q}_{\mathrm{T}}) = \min_{\mathbf{q}_{\mathrm{T},1}+\mathbf{q}_{\mathrm{T},2}=\mathbf{q}_{\mathrm{T}}} \{\max[\, m_{\mathrm{T}}(\mathbf{p}_{\mathrm{T},1}, \mathbf{q}_{\mathrm{T},1}), m_{\mathrm{T}}(\mathbf{p}_{\mathrm{T},2}, \mathbf{q}_{\mathrm{T},2})\,]\},$$

where m_{T} indicates the transverse mass[2], $\mathbf{p}_{\mathrm{T},1}$ and $\mathbf{p}_{\mathrm{T},2}$ are the transverse momentum vectors of the two particles (assumed to be massless), and $\mathbf{q}_{\mathrm{T},1}$ and $\mathbf{q}_{\mathrm{T},2}$ are the unknown transverse momentum vectors of the invisible particles, with $\mathbf{q}_{\mathrm{T}} = \mathbf{q}_{\mathrm{T},1} + \mathbf{q}_{\mathrm{T},2}$. The minimisation is performed over all the possible decompositions of $\mathbf{q}_{\mathrm{T}}$. For $t\bar{t}$ or WW events, where the transverse momenta of the two leptons in each event are taken as $\mathbf{p}_{\mathrm{T},1}$ and $\mathbf{p}_{\mathrm{T},2}$, and $E_{\mathrm{T}}^{\mathrm{miss}}$ as $\mathbf{q}_{\mathrm{T}}$, $m_{\mathrm{T2}}(\ell, \ell, E_{\mathrm{T}}^{\mathrm{miss}})$ is bounded sharply from above by the mass of the W boson [56, 57], while signal events do not respect this bound because of the additional $E_{\mathrm{T}}^{\mathrm{miss}}$ coming from the $\tilde{\chi}_1^0$.

The contribution of SM processes including an on-shell Z boson decaying leptonically is reduced by vetoing events with a same flavour opposite sign lepton pair with 81.2 GeV $< m_{\ell\ell} <$ 101.2 GeV. Furthermore, $\min\{\Delta\phi(\mathrm{jet}_{\mathrm{ISR}}, E_{\mathrm{T}}^{\mathrm{miss}})\}$ is required to be larger than 0.4, to reject events where the $E_{\mathrm{T}}^{\mathrm{miss}}$ comes from mis-measured jets.

Events are required to have at least one jet associated to the ISR system and $\Delta\phi(\mathrm{jet}_{\mathrm{ISR1}}, E_{\mathrm{T}}^{\mathrm{miss}}) > 2$, to ensure to be in the recoiling configuration. Figure 2 shows the expected $E_{\mathrm{T}}^{\mathrm{miss}}$ and leading ISR jet p_{T} distributions for events passing all the requirements described so far.

The $R_{\ell\ell}$ is required to be above 6, to further reduce the SM backgrounds, which peak at lower values. A final signal region (SR) is defined selecting events with $E_{\mathrm{T}}^{\mathrm{miss}} > 350$ GeV, a leading ISR jet with $p_{\mathrm{T}} > 300$ GeV and $m_{\mathrm{T2}} > 100$ GeV. Figure 3 shows the m_{T2} distribution for events passing all the SR requirements except for the one on m_{T2} itself. The main backgrounds that survive the selections are $t\bar{t}$ events that exceed the expected m_{T2} endpoint at the W mass because of the finite detector resolution, and the irreducible $t\bar{t} + Z$ (with $Z \to \nu\nu$) background. This set of selection requirements has been found to be close to optimal when considering only the dataset collected up to LS3 (SR_{300}). The sensitivity expectation in this scenario is expected to be pessimistic, since it has been evaluated using the same response functions derived for the HL–LHC.

A summary of the analysis selections is also presented in Table 1.

Table 1: Summary of the analysis selection criteria (see text for details).

	SR
$m_{\ell\ell}$ [GeV] (SF lepton pairs only)	$81.2 < m_{\ell\ell} < 101.2$
$\min\{\Delta\phi(\mathrm{jet}_{\mathrm{ISR}}, E_{\mathrm{T}}^{\mathrm{miss}})\}$	> 0.4
$\Delta\phi(\mathrm{jet}_{\mathrm{ISR1}}, E_{\mathrm{T}}^{\mathrm{miss}})$	> 2
$R_{\ell\ell}$	> 6
$E_{\mathrm{T}}^{\mathrm{miss}}$ [GeV]	> 350
Leading ISR jet p_{T} [GeV]	> 300
m_{T2} [GeV]	> 100

[2] The transverse mass is defined as $m_{\mathrm{T}} = \sqrt{2|\mathbf{p}_{\mathrm{T},1}||\mathbf{p}_{\mathrm{T},2}|(1 - \cos(\Delta\phi))}$, where $\Delta\phi$ is the angle between the particles with transverse momenta $\mathbf{p}_{\mathrm{T},1}$ and $\mathbf{p}_{\mathrm{T},2}$ in the plane perpendicular to the beam axis.

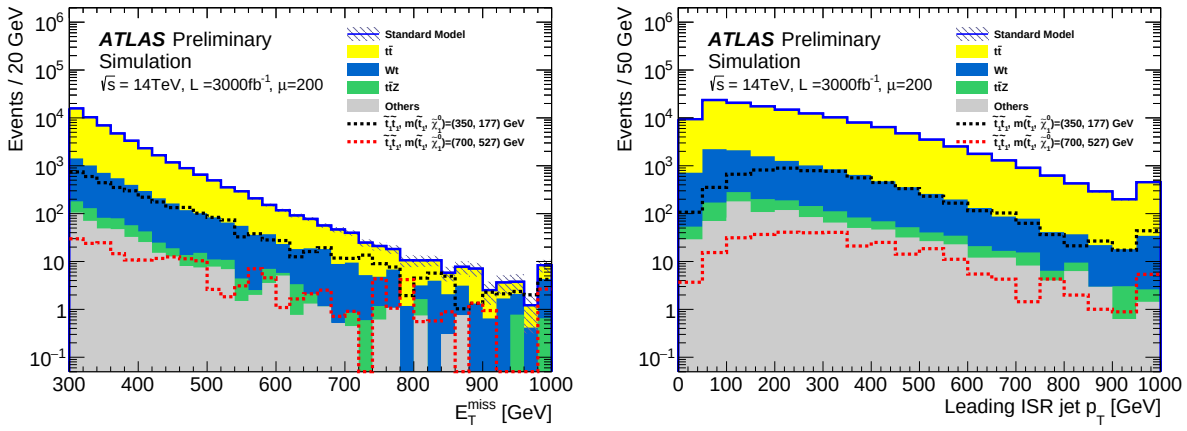

Figure 2: Distributions of $E_{\mathrm{T}}^{\mathrm{miss}}$ (left) and the leading ISR jet p_{T} (right) for events passing the $m_{\ell\ell}$, $\min\{\Delta\phi(\mathrm{jet}_{\mathrm{ISR}}, E_{\mathrm{T}}^{\mathrm{miss}})\}$ and $\Delta\phi(\mathrm{jet}_{\mathrm{ISR1}}, E_{\mathrm{T}}^{\mathrm{miss}})$ requirements described in Section 4 and with $E_{\mathrm{T}}^{\mathrm{miss}}$ >300 GeV. The contributions from all SM backgrounds are shown, and the hashed band represents the statistical uncertainty on the total SM background prediction. The expected distributions for signal models with $m_{\tilde{t}_1}$ = 350 GeV and $m_{\tilde{t}_1}$ = 700 GeV are also shown as dashed lines for comparison.

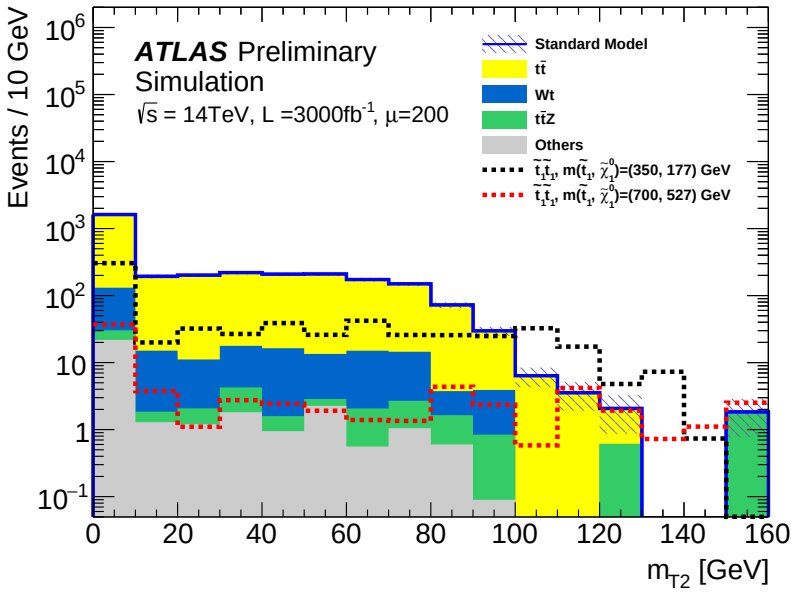

Figure 3: Distributions of m_{T2} for events passing all SR selection requirements, except that on m_{T2} itself. The contributions from all SM backgrounds are shown, and the hashed band represents the statistical uncertainty on the total SM background prediction. The expected distributions for signal models with $m_{\tilde{t}_1}$ = 350 GeV and $m_{\tilde{t}_1}$ = 700 GeV are also shown as dashed lines for comparison.

5 Expected Sensitivity

Table 2 shows the expected yields in the SR for each background source, together with two benchmark signal models.

Table 2: Expected yields in the SR together with their statistical uncertainties, for an integrated luminosity of 3000 fb^{-1}. The expected numbers of events for two signal samples ($m_{\tilde{t}_1}$ = 350 GeV, $m_{\tilde{\chi}_1^0}$ = 177 GeV and $m_{\tilde{t}_1}$ = 700 GeV, $m_{\tilde{\chi}_1^0}$ = 527 GeV) are also reported.

	SR
Expected Standard Model	13.8 ± 6.5
$t\bar{t}$	11.4 ± 5.1
$t\bar{t} + Z$	2.4 ± 1.5
Others	$0.0^{+1.8}_{-0.0}$
$\tilde{t}_1\,\tilde{t}_1\; m(\tilde{t}_1, \tilde{\chi}_1^0) = (350, 177)$ GeV	62.7 ± 7.5
$\tilde{t}_1\,\tilde{t}_1\; m(\tilde{t}_1, \tilde{\chi}_1^0) = (700, 527)$ GeV	11.0 ± 2.0

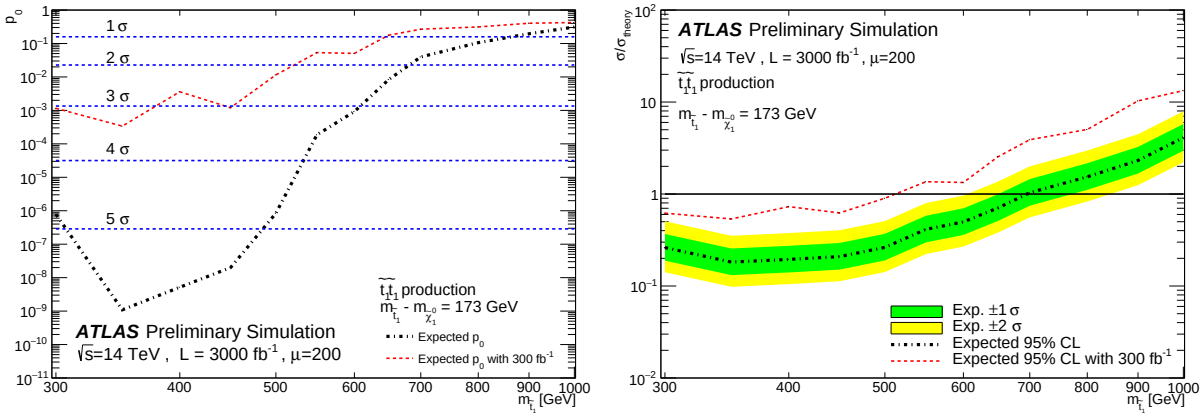

Figure 4: Expected compatibility, in terms of p-value p_0, with the background-only hypothesis (left) and exclusion limits at 95% CL shown as the ratio between the cross-section limit σ and the nominal NLO+NLL prediction σ_{theory} (right) from the analysis of 3000 fb^{-1}of 14 TeV proton-proton collision data as a function of the $\tilde{t}_1$ mass, for $m_{\tilde{t}_1} - m_{\tilde{\chi}_1^0} = 173$ GeV and assuming BR($\tilde{t}_1 \to t\tilde{\chi}_1^0$) = 1. The shaded bands show the effect on the limit of respectively one and two sigma variations on the background prediction. The sensitivity from the analysis of 300 fb^{-1}of 14 TeV collision data is also shown as a red dashed line for comparison.

The HistFitter framework [58], which utilises a profile-likelihood-ratio test statistics [59], is used to compute expected exclusion limits with the CL$_s$ prescription [60] assuming a 30% systematic uncertainty on the background expectation.

Scans of expected discovery significance and 95% CL limits are shown in Figure 4 as a function of the $\tilde{t}_1$ mass. Simplified models of top squark production are considered, in which the $\tilde{t}_1$ decays with 100% branching ratio into $t\tilde{\chi}_1^0$. The 5σ discovery potential for the full HL-LHC dataset is expected to extend up to $m_{\tilde{t}_1}$ = 480 GeV, while in the absence of a signal, $\tilde{t}_1$ masses up to 700 GeV are expected to be excluded at 95% CL.

6 Conclusion

The sensitivity to heavy SUSY particles will be increased significantly with the analysis of ATLAS data collected in proton-proton collisions at the LHC design centre-of-mass-energy of $\sqrt{s} = 14$ TeV. Feasibility studies on benchmark SUSY scenarios for direct top squark production are carried out with MC simulated events generated at $\sqrt{s} = 14$ TeV, and with corrections accounting for the detector response applied to the generator-level particles. A dataset of 3000 fb^{-1} extends the discovery potential for $\tilde{t}_1\tilde{t}_1$ production up to 480 GeV and the exclusion sensitivity up to masses of about 700 GeV, assuming $\tilde{t}_1 \to t\tilde{\chi}_1^0$ and $m_{\tilde{t}_1} - m_{\tilde{\chi}_1^0} = 173$ GeV with both top quarks decaying leptonically. The fully hadronic and semi-leptonic channels, which have not been considered in this study, are likely to further extend this reach. Future improvements in the understanding of experimental and theoretical systematic uncertainties on the SM backgrounds would provide additional gains in sensitivity.

References

[1] Yu. A. Golfand and E. P. Likhtman,
Extension of the Algebra of Poincare Group Generators and Violation of P Invariance,
JETP Lett. **13** (1971) 323, [Pisma Zh. Eksp. Teor. Fiz.13,452(1971)].

[2] D. V. Volkov and V. P. Akulov, *Is the Neutrino a Goldstone Particle?*, Phys. Lett. **B46** (1973) 109.

[3] J. Wess and B. Zumino, *Supergauge Transformations in Four-Dimensions*,
Nucl. Phys. **B70** (1974) 39.

[4] J. Wess and B. Zumino, *Supergauge Invariant Extension of Quantum Electrodynamics*,
Nucl. Phys. **B78** (1974) 1.

[5] S. Ferrara and B. Zumino, *Supergauge Invariant Yang-Mills Theories*,
Nucl. Phys. **B79** (1974) 413.

[6] A. Salam and J. A. Strathdee, *Supersymmetry and Nonabelian Gauges*,
Phys. Lett. **B51** (1974) 353.

[7] G. R. Farrar and P. Fayet, *Phenomenology of the Production, Decay, and Detection of New Hadronic States Associated with Supersymmetry*, Phys. Lett. **B76** (1978) 575.

[8] N. Sakai, *Naturalness in Supersymmetric Guts*, Z. Phys. **C11** (1981) 153.

[9] S. Dimopoulos, S. Raby and F. Wilczek, *Supersymmetry and the Scale of Unification*,
Phys. Rev. **D24** (1981) 1681.

[10] L. E. Ibanez and G. G. Ross, *Low-Energy Predictions in Supersymmetric Grand Unified Theories*,
Phys. Lett. **B105** (1981) 439.

[11] S. Dimopoulos and H. Georgi, *Softly Broken Supersymmetry and SU(5)*,
Nucl. Phys. **B193** (1981) 150.

[12] R. Barbieri and G. F. Giudice, *Upper Bounds on Supersymmetric Particle Masses*,
Nucl. Phys. **B306** (1988) 63.

[13] B. de Carlos and J. A. Casas, *One loop analysis of the electroweak breaking in supersymmetric models and the fine tuning problem*, Phys. Lett. **B309** (1993) 320, arXiv: hep-ph/9303291.

[14] K. Inoue et al., *Aspects of Grand Unified Models with Softly Broken Supersymmetry*,
Prog. Theor. Phys. **68** (1982) 927, [Erratum: Prog. Theor. Phys. **70** (1983) 330].

[15] J. R. Ellis and S. Rudaz, *Search for Supersymmetry in Toponium Decays*,
Phys. Lett. **B128** (1983) 248.

[16] ATLAS Collaboration, *ATLAS Run 1 searches for direct pair production of third-generation squarks at the Large Hadron Collider*,
Eur. Phys. J. **C75** (2015) 510, [Erratum: Eur. Phys. J.C76,no.3,153(2016)],
arXiv: 1506.08616 [hep-ex].

[17] ATLAS Collaboration, *Measurement of Spin Correlation in Top–Antitop Quark Events and Search for Top Squark Pair Production in pp Collisions at* $\sqrt{s} = 8$ *TeV Using the ATLAS Detector*,
Phys. Rev. Lett. **114** (2015) 142001, arXiv: 1412.4742 [hep-ex].

[18] ATLAS Collaboration, *Search for direct top squark pair production and dark matter production in final states with two leptons in* $\sqrt{s} = 13$ *TeV pp collisions using 13.3* fb^{-1} *of ATLAS data*,
ATLAS-CONF-2016-076, 2016, URL: https://cds.cern.ch/record/2206249.

[19] ATLAS Collaboration, *Search for top squarks in final states with one isolated lepton, jets, and missing transverse momentum in $\sqrt{s} = 13$ TeV pp collisions with the ATLAS detector*, ATLAS-CONF-2016-050, 2016, URL: https://cds.cern.ch/record/2206132.

[20] ATLAS Collaboration, *Search for the Supersymmetric Partner of the Top Quark in the Jets+Emiss Final State at sqrt(s) = 13 TeV*, ATLAS-CONF-2016-077, 2016, URL: https://cds.cern.ch/record/2206250.

[21] CMS Collaboration, *Search for top-squark pair production in the single-lepton final state in pp collisions at $\sqrt{s} = 8$ TeV*, Eur. Phys. J. C **73** (2013) 2677, arXiv: 1308.1586 [hep-ex].

[22] CMS Collaboration, *Search for supersymmetry using razor variables in events with b-tagged jets in pp collisions at $\sqrt{s} = 8$ TeV*, Phys. Rev. D **91** (2015) 052018, arXiv: 1502.00300 [hep-ex].

[23] CMS Collaboration, *Searches for supersymmetry using the M_{T2} variable in hadronic events produced in pp collisions at 8 TeV*, JHEP **05** (2015) 078, arXiv: 1502.04358 [hep-ex].

[24] CMS Collaboration, *Search for supersymmetry in events with soft leptons, low jet multiplicity, and missing transverse momentum in proton-proton collisions at $\sqrt{s}$=8 TeV*, Submitted to Phys. Lett. B (2015), arXiv: 1512.08002 [hep-ex].

[25] CMS Collaboration, *Search for direct pair production of scalar top quarks in the single- and dilepton channels in proton-proton collisions at $\sqrt{s}$=8 TeV*, Submitted to JHEP (2016), arXiv: 1602.03169 [hep-ex].

[26] CMS Collaboration, *A Search for Scalar Top Quark Production and Decay to All Hadronic Final States in pp Collisions at $\sqrt{s}$=8 TeV*, CMS-PAS-SUS-13-023, 2015, URL: https://cds.cern.ch/record/2044441.

[27] ATLAS Collaboration, *Prospects for benchmark Supersymmetry searches at the high luminosity LHC with the ATLAS Detector*, ATL-PHYS-PUB-2013-011, 2013, URL: http://cdsweb.cern.ch/record/1604505.

[28] ATLAS Collaboration, *The ATLAS Experiment at the CERN Large Hadron Collider*, JINST **3** (2008) S08003.

[29] C. ATLAS, *Letter of Intent for the Phase-II Upgrade of the ATLAS Experiment*, Draft version for comments, 2012, URL: https://cds.cern.ch/record/1502664.

[30] *ATLAS Phase-II Upgrade Scoping Document*, 2015, URL: https://cds.cern.ch/record/2055248.

[31] ATLAS Collaboration, *Simulation of top-quark production for the ATLAS experiment at $\sqrt{s} = 13$ TeV*, ATL-PHYS-PUB-2016-004, 2016, URL: http://cdsweb.cern.ch/record/2120417.

[32] S. Frixione, P. Nason and G. Ridolfi, *A Positive-weight next-to-leading-order Monte Carlo for heavy flavour hadroproduction*, JHEP **09** (2007) 126, arXiv: 0707.3088 [hep-ph].

[33] P. Nason, *A New method for combining NLO QCD with shower Monte Carlo algorithms*, JHEP **11** (2004) 040, arXiv: hep-ph/0409146 [hep-ph].

[34] S. Frixione, P. Nason and C. Oleari, *Matching NLO QCD computations with Parton Shower simulations: the POWHEG method*, JHEP **11** (2007) 070, arXiv: 0709.2092 [hep-ph].

[35] T. Sjöstrand, S. Mrenna and P. Z. Skands, *A Brief Introduction to PYTHIA 8.1*, Comput. Phys. Commun. **178** (2008) 852, arXiv: 0710.3820 [hep-ph].

[36] ATLAS Collaboration, *ATLAS Pythia8 tunes to 7 TeV data*, ATL-PHYS-PUB-2014-021, 2014, URL: http://cds.cern.ch/record/1966419.

[37] H.-L. Lai et al., *New parton distributions for collider physics*, Phys.Rev. **D82** (2010) 074024, arXiv: 1007.2241 [hep-ph].

[38] M. Czakon and A. Mitov, *Top++: A Program for the Calculation of the Top-Pair Cross-Section at Hadron Colliders*, Comput.Phys.Commun. **185** (2014) 2930, arXiv: 1112.5675 [hep-ph].

[39] J. Alwall et al., *The automated computation of tree-level and next-to-leading order differential cross sections, and their matching to parton shower simulations*, JHEP **07** (2014) 079, arXiv: 1405.0301 [hep-ph].

[40] ATLAS Collaboration, *Modelling of the $t\bar{t}H$ and $t\bar{t}V$ ($V = W, Z$) processes for $\sqrt{s} = 13$ TeV ATLAS analyses*, ATL-PHYS-PUB-2015-022, 2016, URL: http://cds.cern.ch/record/2120826.

[41] R. D. Ball et al., *Parton distributions with LHC data*, Nucl. Phys. **B867** (2013) 244, arXiv: 1207.1303 [hep-ph].

[42] T. Gleisberg et al., *Event generation with SHERPA 1.1*, JHEP **02** (2009) 007, arXiv: 0811.4622 [hep-ph].

[43] ATLAS Collaboration, *Multi-Boson Simulation for 13 TeV ATLAS Analyses*, ATL-PHYS-PUB-2016-002, 2016, URL: http://cds.cern.ch/record/2119986.

[44] G. Corcella et al., *HERWIG 6: An Event generator for hadron emission reactions with interfering gluons (including supersymmetric processes)*, JHEP **01** (2001) 010, arXiv: hep-ph/0011363.

[45] J. Pumplin et al., *New generation of parton distributions with uncertainties from global QCD analysis*, JHEP **07** (2002) 012, arXiv: hep-ph/0201195.

[46] LHC Higgs Cross Section Working Group, *Handbook of LHC Higgs Cross Sections: 2. Differential Distributions*, CERN-2012-002 (CERN, Geneva, 2012), arXiv: 1201.3084 [hep-ph].

[47] L. Lönnblad and S. Prestel, *Matching Tree-Level Matrix Elements with Interleaved Showers*, JHEP **03** (2012) 019, arXiv: 1109.4829 [hep-ph].

[48] W. Beenakker et al., *Stop production at hadron colliders*, Nucl. Phys. **B515** (1998) 3, eprint: hep-ph/9710451.

[49] W. Beenakker et al., *Supersymmetric top and bottom squark production at hadron colliders*, JHEP. **1008** (2010) 098, eprint: arXiv:1006.4771[hep-ph].

[50] W. Beenakker et al., *Squark and gluino hadroproduction*, Int.J.Mod.Phys. **A26** (2011) 2637, arXiv: 1105.1110 [hep-ph].

[51] M. Krämer et al., *Supersymmetry production cross sections in pp collisions at $\sqrt{s} = 7$ TeV*, (2012), arXiv: 1206.2892 [hep-ph].

[52] D. J. Lange, *The EvtGen particle decay simulation package*, Nucl. Instrum. Meth. **A462** (2001) 152.

[53] ATLAS Collaboration, *Performance of b-Jet Identification in the ATLAS Experiment*, (2015), arXiv: 1512.01094 [hep-ex].

[54] C. G. Lester and D. J. Summers, *Measuring masses of semiinvisibly decaying particles pair produced at hadron colliders*, Phys. Lett. B **463** (1999) 99, arXiv: hep-ph/9906349.

[55] A. Barr, C. Lester and P. Stephens, *m(T2) : The Truth behind the glamour*, J. Phys. G **29** (2003) 2343, arXiv: hep-ph/0304226.

[56] W. S. Cho et al., *Measuring superparticle masses at hadron collider using the transverse mass kink*, JHEP **02** (2008) 035, arXiv: 0711.4526 [hep-ph].

[57] M. Burns et al., *Using Subsystem MT2 for Complete Mass Determinations in Decay Chains with Missing Energy at Hadron Colliders*, JHEP **03** (2009) 143, arXiv: 0810.5576 [hep-ph].

[58] M. Baak et al., *HistFitter software framework for statistical data analysis*, Eur. Phys. J. **C75** (2015) 153, arXiv: 1410.1280 [hep-ex].

[59] G. Cowan et al., *Asymptotic formulae for likelihood-based tests of new physics*, Eur. Phys. J. **C71** (2011) 1554, [Erratum: Eur. Phys. J. **C73** (2013) 2501], arXiv: 1007.1727 [physics.data-an].

[60] A. L. Read, *Presentation of search results: the CL s technique*, Journal of Physics G: Nuclear and Particle Physics **28** (2002) 2693.